land

MDPI

Article

The Application of Soil Erosion Models of an Agroforestry Basin under Mediterranean Conditions from a Geotechnical Point of View

Ana Paula Leite [1], António Canatário Duarte [2,3], Leonardo Marchiori [4,*], Maria Vitoria Morais [4], André Studart [4] and Victor Cavaleiro [4,*]

[1] Lisbon and Tagus Valley Regional Coordination and Development Commission, 1250-009 Lisbon, Portugal; anappleite@hotmail.com
[2] School of Agriculture, Polytechnic Institute of Castelo Branco, 6000-084 Castelo Branco, Portugal; acduarte@ipcb.pt
[3] CERNAS, Polytechnic Institute of Castelo Branco, 6000-084 Castelo Branco, Portugal
[4] GeoBioTec, Department of Civil Engineering and Architecture, University of Beira Interior, 6201-001 Covilhã, Portugal; vitoria.morais@ubi.pt (M.V.M.); andre.studart@ubi.pt (A.S.)
* Correspondence: leonardo.marchiori@ubi.pt (L.M.); victorc@ubi.pt (V.C.)

Abstract: Soil erosion has been causing an imbalance in nature and the environment. It is mainly caused naturally but is also due to human interventions leading to desertification and possible contamination. Therefore, engineering, geography, and cartography have been allies in applying erosion models to predict, address, and remediate the impacts. Therefore, the Revised Universal Soil Loss Equation (RUSLE) and Soil and Water Assessment Tool (SWAT) linked to Geographic Information Systems (GISs) could boost decision making as tools to mitigate issues. This study applies the RUSLE and SWAT models from a geotechnical point of view to analyze a sub-watershed at Idanha-a-Nova (Portugal) over 4 years, showing a predominant erosion risk class with losses lower than 5 t.ha^{-1}.year^{-1} (60 to 86%), characterized as very low risk. The modeling permitted the development of soils erosion susceptibility charts, in addition to material availability and the suitability for construction areas, exposing a replicable methodology that could contribute to minimizing environmental impacts while encouraging a more intelligent use of the land towards a greener exploration.

Keywords: RUSLE; SWAT; GIS; soil erosion; susceptibility chart; sustainable development

Citation: Leite, A.P.; Duarte, A.C.; Marchiori, L.; Morais, M.V.; Studart, A.; Cavaleiro, V. The Application of Soil Erosion Models of an Agroforestry Basin under Mediterranean Conditions from a Geotechnical Point of View. *Land* **2024**, *13*, 1613. https://doi.org/10.3390/land13101613

Academic Editors: Asim Biswas, Jianjun Cao, Dewei Yang and Jian Zhang

Received: 1 August 2024
Revised: 16 September 2024
Accepted: 30 September 2024
Published: 4 October 2024

1. Introduction

Soil erosion by water has always occurred on the Earth's surface, being one of the main shaping forces of the planet's crust. Considering that erosion is a natural process, it can be responsible for soil impoverishment due to alluvial deposits on the banks of water courses [1]. Particularly, geological erosion occurs without human intervention due to multiple activities, having the capacity to restore previous balances [2]. However, human activity can increase soil erosion due to agricultural practice, mining activities, and deforestation [3].

Thus, water erosion represents a cost for agriculture, as it decreases the land's productivity, impacting nutrients and organic matter. In addition, chemicals, such as fertilizers, are used to maintain a certain productive capacity of the soil [4], although they impact the soils' chemical composition, affecting the fauna and flora. Such impacts harm nature's sustainability and hinder greener measures, impacting the long-term viability of such a model, possibly leading to desertification [5] and changes in the region's climate. Gómez et al. [6] and Prosdocimi et al. [7] argue that Mediterranean erosion by water is due to the climate, mainly the long and dry summer, lowering the maintenance of vegetation

cover whilst increasing heavy rains in the late summer and during autumn, adding erosive potential [8].

In addition, contamination can happen, caused by sediments dragged from agricultural plots, which can be present in the physical and chemical dimensions [9]. Physical refers to the loss of soil particles from its surface layer, leading to excessive levels of turbidity and ecological repercussions on aquatic ecosystems [10]. As a consequence, the sedimentation rate increases, changing hydraulic characteristics, impacting floods, and possibly clogging reservoirs and reducing their water storage capacity [11]. The chemical dimension mainly concerns active clays from sediments, transporting heavy metals, pesticides, or micropollutants to the environment.

Studies have also shown that organic nitrogen and phosphorus are transported within lime and clays [12]. Furthermore, the Portuguese National Water Plan [13] indicated that phosphorus is the determining element in the eutrophication of reservoirs, which can lead to an increase in tributary loads for correction of this element. Water erosion represents a decrease in the potential for carbon sequestration, one of the most important elements in the contribution to the greenhouse effect in the Earth's atmosphere [14,15].

In the European Union (EU), it is estimated that 52 million hectares of soil, equivalent to more than 16% of the total land surface, is affected by degradation processes. Outside the EU, this percentage is around 35% according to the world map of human-induced soil erosion [16,17]. The Food and Agriculture Organization (FAO) [18] and UE reveal that the main cause of soil degradation is related to inadequate management, estimating that 115 million hectares, equivalent to 12% of the European territory, are subject to water erosion and that 45% of European soil will have too low an organic matter content, mainly affecting southern European countries [19]. In addition, China is the first ranked country with rural populations affected by land degradation, with around 500 million people affected [17]. Such a high number points to the need to take effective measures to protect soil as a natural resource [19,20].

Therefore, simulation models have contributed effectively to the mitigation of water erosion due to their efficiency in defining soil conservation strategies [21–23]. Soil models can simulate a temporal dimension—year, day, rainfall—and territorial dimension, such as an agricultural parcel, slope, and watershed. These models can process data of different natures with a varied database, allowing the studies of alternative ways to use land whilst ensuring its sustainability [24,25]. In addition, such models support GIS application [26]. Several models are dedicated exclusively to simulating the erosion process or more comprehensively to the diffuse pollution process: the Annualized Agricultural Non-Point Source (AnnAGNPS) [27], Soil and Water Assessment Tool (SWAT) [28], Chemicals, Runoff and Erosion from Agricultural Management Systems (CREAMS) [29], Water Erosion Prediction Project (WEPP) [30], EUROpean Soil Erosion Model (EUROSEM) [24], Erosion Productivity Impact Calculator (EPIC) [31], Universal Soil Loss Equation (USLE) [32], Revised Universal Soil Loss Equation (RUSLE) [33], and KINematic Runoff and EROSion Model (KINEROS2) [34].

The main objectives of this work are to apply two water erosion models, one more simplified and universal—RUSLE—and the other more complex—SWAT—to GIS to draw inferences about the areas with a risk of erosion in terms of temporal and spatial factors within the studied watershed. Then, we simulate different scenarios linked to different land occupations and climate to verify the impact on the studied sub-basin to improve its management, which can serve as a prototype for other regions of the country. In addition, identifying areas that are at risk of erosion within the sub-watershed and creating erosion susceptibility charts within the study area is the final objective. The present study highlights the importance of analysis and tool verification for increasing the decision-making capacity to correctly plan and manage usable land.

The presented charts help identify highly susceptible areas for erosion, allowing for targeted management measures and sustainable practices and identifying risk areas for policymakers for zoning regulations. Furthermore, this study contributes to risk assess-

ment and mitigation, aiming at the protection of human life and existing infrastructure. Economically, this study supports cost-effective land management by minimizing environmental impacts, ensuring the long-term stability and safety of construction projects through informed site selection.

2. Materials and Methods

The studied watershed is in the municipality of Idanha-a-Nova (Figure 1), Portugal, which is included in the Hydro-Agricultural Development of Campina da Idanha, bordering Spain on the east and the Tagus International Natural Park on the south. The studied basin has an area of 189 ha, presents a third-order fluvial hierarchy (drained by a set of 28 water lines), and a drainage density of 12.2 m/ha. This study was carried out across 4 years (2009–2013), being currently monitored.

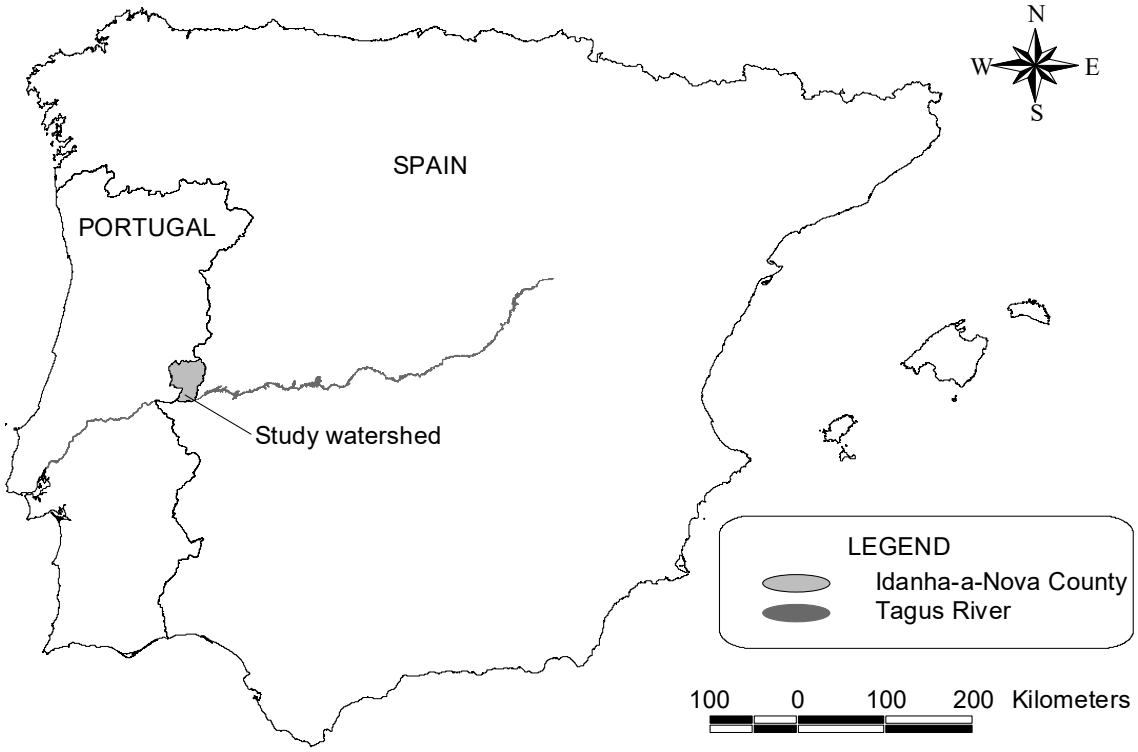

Figure 1. Location of the studied watershed.

2.1. Basin Characteristics

The geotechnical mapping was developed for the characterization of the soil and subsoil looking to improve the management of the territory. The definition of the criteria for land occupation and geotechnical units allows an adequate amount of civil engineering works, mitigating disasters [35,36]. The inventory of natural resources, geological heritage, and areas of natural risk are factors included, and the objectives of geological–geotechnical maps are directed towards the following [37,38] purposes:

- Better use of available physical space;
- Environmental conservation and protection of natural resources;
- Establishment of technical criteria for land use and degraded areas recovery;
- Optimization of public and private resources;
- Population and infrastructures maintenance through the prediction and prevention of geological hazards;
- Guidance of specific studies and tests for engineering projects.

The use of the patterns–units–components–evaluation (PUCE) methodology [39] was also applied to support these objectives, defining several Earth classes. These classes are

established by analyzing several parameters, namely, topography, nature and structure of the material, erosion form, vegetation, and land use [40]. The hydrological station was installed at the outlet of the watershed, consisting of a long-throated flume, with a controlled triangular section for small water depths and triangular and trapezoidal for larger water depths, designed and calibrated according to [41]. The ultrasonic sensor was connected to a datalogger to measure and record water depth (Figure 2), and monitor discharge and sediment production.

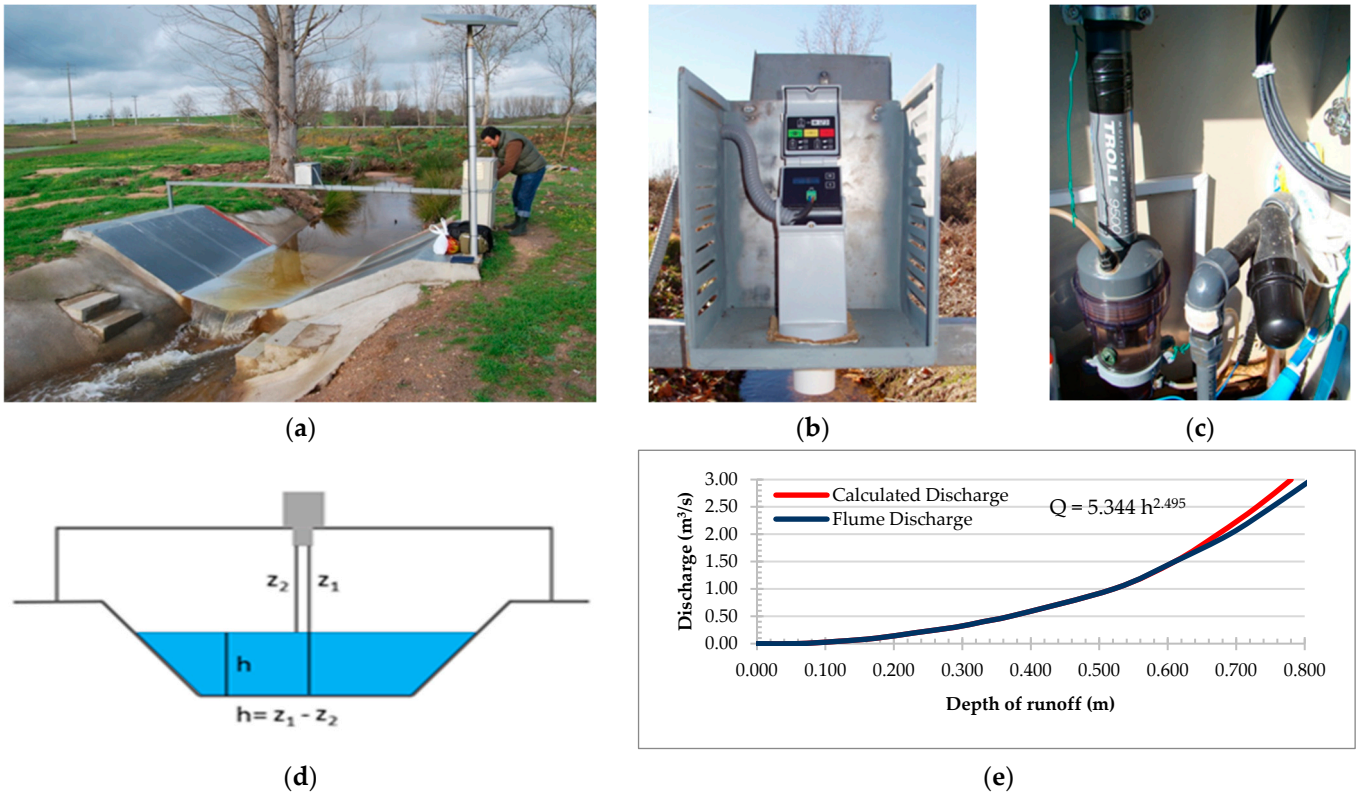

Figure 2. General view of hydrometric and water quality station (**a**), ultrasonic sensor to evaluate the flow depth (**b**), multiparameter probe inside of a cup where the water is delivered to evaluation its quality (**c**), schematic of the runoff depth evaluation by using a flume and an ultrasonic sensor (**d**), and discharge curve of the flume (calculated, blue line; exponential adjustment, red line) (**e**).

2.2. Hydrogeological and Geomorphological Characterization

Figure 3 exposes the general topography of the basin with the water separation lines. The elevations vary between 248 m, in the extreme NE, in a plateau area, and 212 m in the reference section of the basin. The most representative slopes vary between 0 and 4%, fitting in a slightly waved area with some greater slopes.

Many of the soil characteristics of this hydrographic basin were determined by geological phenomena that are related to the deposition of coarse elements at higher altitudes from the tributary channels of Tagus River. These soils have a very high percentage of coarse elements, they occupy a large part of the higher altitude areas of the basin, and, due to their pedogenesis, they are Cambisols [18]. In areas where this deposition phenomenon was very accentuated, or where there was later accentuated transport of coarse elements, the predominant pedogenetic process is not deposition, but alteration and transport within the soil profile. These processes are related to the other significant part of soil in the basin, the Luvisols [18].

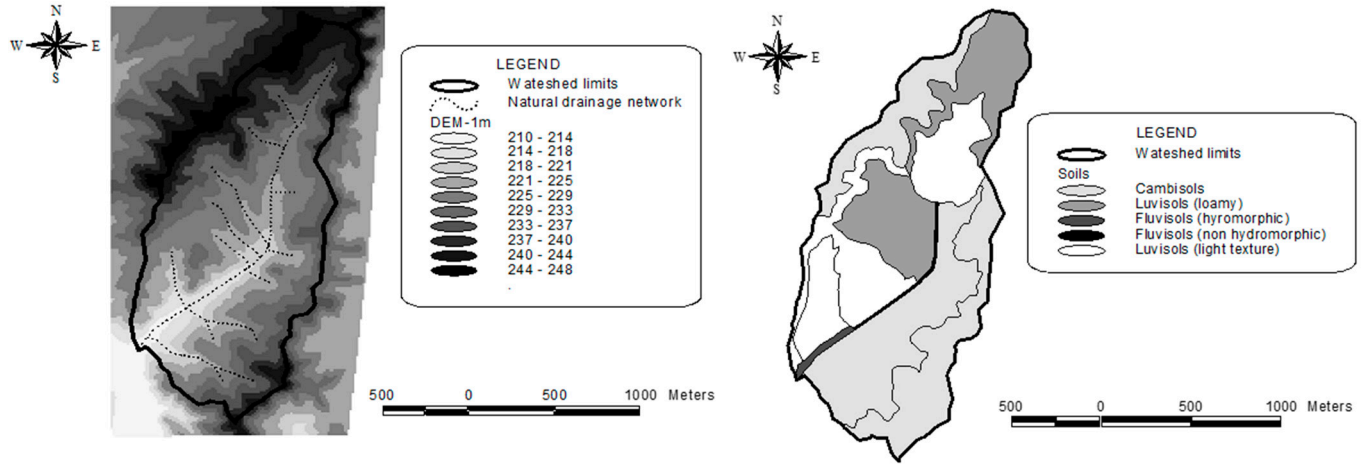

Figure 3. Topography and natural drainage network (**a**), and soil classes of the study watershed (FAO nomenclature) (**b**).

The pedological reality of the basin is dominated by Cambisols, which correspond mainly to plateau deposits of the tributary water lines of the Tagus River with very heterogeneous profiles, and Luvisols located at lower altitudes. There is another category that has little representation in the basin, the Fluvisols, presented on the banks of watercourses to varying extents. The climate of the area is typically continental Mediterranean, averaging an annual rainfall of 624 mm, and daily temperatures that vary between 8.3 °C in January and 24.5 °C in August [42], typical for countryside areas. The climate of the area is also marked by a strong randomness of the climatic parameters.

According to the Köppen climate classification, the thermopluviometric characteristics correspond to those of the *Csa* climate type [43]. The data informed us that the average annual rainfall was 584 mm (data series 1981–2010), with a dry and hot period during the summer, and daily temperature fluctuating between 7.3 °C in January and 25.8 °C in July, with a thermal amplitude typical of countryside areas.

The basin presents, in terms of its use, three quite distinct zones: a zone of nonagricultural use (holm oaks and cork oaks scattered with herbaceous and shrub vegetation), a zone of intensive agricultural use (irrigated corn), and a zone with smaller fields with miscellaneous crops use (meadow, sorghum, oat). Shown in Figure 4 is the land uses verified in the 4 years of this study.

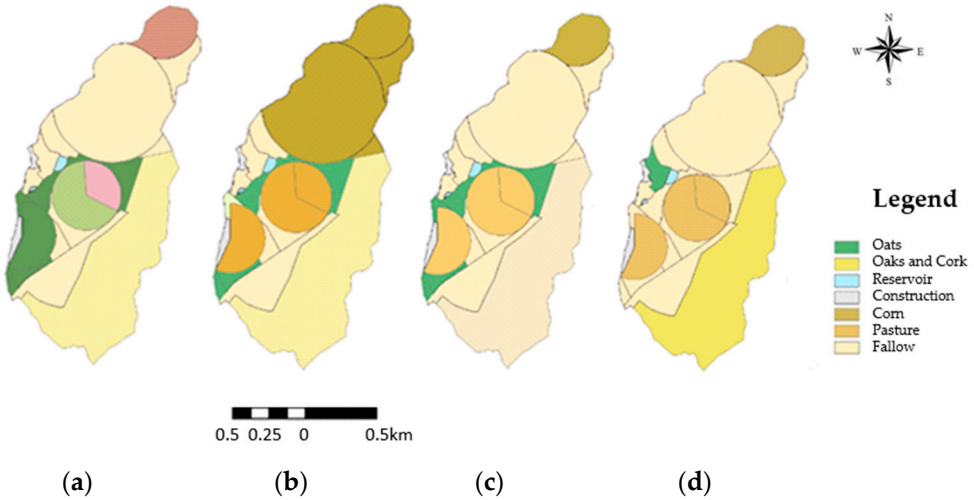

Figure 4. Land use in the study basin in the 1st (**a**), 2nd (**b**), 3rd (**c**), and 4th (**d**) years.

Regarding the regional geological framework, the studied area is part of the Hesperic Massif, which constitutes the Pre-Cambrian/Paleozoic basement of the Iberian Peninsula, corresponding to an ancient and relatively rigid continental crust, definitively consolidated at the end of the Paleozoic. In the heart of the Hesperic Massif, the area is in the southwestern edge of the Central Iberian Zone, which occupies the central and western part of the Peninsula [44]. This area is formed, mostly, by sediments of the "flysh" Schist-Grauvach Complex called the Beiras Group. This complex is made up of granitoid rocks of great textural and mineralogical variety and veins of different nature [45].

With regard to geological and geomorphological characterization, there are some studies worth mentioning. The authors of [46] carried out extensive work on Ordovician materials from Beira Baixa; the authors of [47–52] developed a vast amount of work on both geomorphology and the Cenozoic materials of Beira Baixa; more recent works [53,54], carried out detailed studies in this region on the Spanish side; the authors of [55] contributed to a greater knowledge of the formations along the border; finally, the authors of [56] devoted detailed work to the substrate formations in this region.

2.3. Soil Loss Calculations

The drainage network was digitalized from the military chart of Portugal, Series M888, with a scale of 1:25.000. The database for the preparation of the digital elevated models (DEMs) were the topographic maps with a scale of 1:2500 (Folios 6I and 7I), prepared by the former Junta Autónoma das Obras de Hidráulica Agrícola in 1947 for the Idanha-a-Nova region, on the draft project for the Idanha Countryside Irrigation Zone. Regarding parameters assessment, hydrogeological and geomorphological characterization were used for modeling, namely, soil data comprising physicochemical and biological aspects, in addition to agricultural, climate, topographic, and hydrological, as mentioned above.

RUSLE methodology [33], in general, uses its equation modifying the antecedent, USLE, to calculate the average annual soil loss (A). Here, RUSLE was modified to be applied at the basin scale and in continuous simulation processes, as [57] indicated. The effect of the topography of a slope on water erosion is represented by two factors: the length factor (L) and the slope factor (S) of the slope, both represented as single LS factor, estimated for each catchment cell in the AnnAGNPS AgFlow module, for each length and elevation difference. Soil cover factor (C) represents the effect of crops and agricultural practices on the rate of erosion, and conservative practices factor (P) reflects the effect of practices considered conservative that impact surface runoff. Both are presented together as the CP factor. The soil loss rate (SLR) corresponds to the relationship between the losses of soil produced in a certain situation and those that would be obtained with reference conditions. The RUSLE proposes the calculation of SLR for time periods of 15 days, considering that the most important factors remain constant during that period [33]. The determination of this factor follows the steps described in [33,58].

RUSLE was designed to predict over a period the A, following Equation (1) and the abovementioned factors.

$$A = R \times K \times LS \times CP, \quad (1)$$

where A ($t.ha^{-1}.year^{-1}$) is the average annual soil loss, R ($MJ.mm.ha^{-1}.h^{-1}$) is the runoff erosivity factor, K ($t.h.MJ^{-1}.mm^{-1}$) is the soil erodibility, LS (-) comprises length (L) and slope (S) factors together, like CP (-) with cover (C) and practice (P) factors; the last two are dimensionless.

The sediments that the model predicts are based on the Modified Universal Soil Equation (MUSLE) [59], which is the adjusted equation used in hydrographic basins, and is based on surface runoff and maximum runoff in addition to other variables such as cover, soil, and slope. This is expressed as Equation (2).

$$Sed = 11.8 \times \left(Q_{sur} \times Q_{peak} \times Area_{hru}\right)^{0.56} \times K_{usle} \times C_{usle} \times P_{usle} \times L_{usle}, \quad (2)$$

where Sed (t) is the production of sediment in one day, Q_{sur} (mm) is surface runoff, Q_{peak} ($m^3.s^{-1}$) is peak flow, $Area_{hru}$ (ha) is area of homogeneous hydrological response units, K_{usle} is soil erodibility factor, C_{usle} is coverage factor, P_{usle} is soil conservation practices factor, and LS_{usle} is the topographic factor of the USLE.

The factor that considers the effect of precipitation on the erosive process is the erosion index (EI), and it is calculated for a given distribution of precipitation, which is the same as that used in the CREAMS model [29].

According to the classification [60], the SWAT model is a mathematical model, being physically based on deterministic properties, leading to a continuous model, not designed to make forecasts for individual storms [61]. The model is based on hydrology and description of erosion processes with inputs, providing results in a spatially distributed way for a particular hydrographic basin, facing continuous simulations over time, regarding various precipitation events. The actualization of the model Simulator for Water Resources in Rural Basins (SWRRB) was developed by Williams [31] and his collaborators [28].

The SWAT integrates climate, soil, topography, vegetation, and soil management practices variables to predict changes that may occur in a watershed. The parameters' calibration was initiated by the flow, then the sediment production and water quality [62], both according to the guidelines [63], in order to improve the efficiency of the model. Regarding the software's versions, the following programs were used: ArcGIS 10.8, SWAT2009, and WGN Excel Macro 2007.

3. Results

3.1. RUSLE Application

Table 1 summarizes the calculation of the RUSLE factor within different method proposed by author after mentioned for each factor.

Table 1. Results of soil loss simulations and annual potential soil loss classes according to the different methods of calculating the RUSLE factors.

Method *	Cell Dimension	Annual Soil Loss (A) ($t.ha^{-1}.year^{-1}$)			Area (%) by Erosion Risk Class (t/ha)				
		Average	Standard Deviation	Max	<5	5–12	12–50	100–200	>200
1	5 m	13.06	55.23	1512.50	76.99	10.42	7.23	1.50	2.37
	10 m	13.00	52.24	1120.60	76.88	10.41	7.27	1.49	2.37
2	5 m	18.89	77.78	1520.97	73.87	11.41	7.17	1.99	3.20
	10 m	18.85	75.31	1512.50	73.71	11.55	7.12	1.95	3.25
3	5 m	39.57	131.97	1921.53	49.89	20.18	20.44	2.16	1.61
	10 m	39.80	133.14	1847.85	49.99	20.13	20.38	2.19	1.61
4	5 m	1.42	6.24	222.71	93.43	4.91	1.37	0.19	0.09
	10 m	1.43	6.19	222.71	93.21	5.17	1.32	0.21	0.08
5	5 m	3.12	5.97	76.99	84.94	8.48	6.46	0.12	0.00
	10 m	3.14	6.00	76.99	84.93	8.45	6.50	0.12	0.00
6	5 m	3.54	6.00	76.99	81.80	11.26	6.82	0.12	0.00
	10 m	3.56	6.03	76.99	81.82	11.19	6.87	0.12	0.00

* Scenarios. 1—R (30 years) × K1 (Equation (4), 15 profiles) × LS (Equation (6)) × CP (Year 1). 2—R (30 years) × K1 (Equation (4), 8 profiles) × LS (Equation (6)) × CP (Year 1). 3—R (30 years) × K1 (Equation (4), 15 profiles) × LS (Equation (7)) × CP (Year 1). 4—R (30 years) × K2 (Equation (5), 15 profiles) × LS (Equation (6)) × CP (Year 1). 5—R (30 years) × K2 (Equation (5), 15 profiles) × LS (Equation (7)) × CP (Year 1). 6—R (30 years) × K2 (Equation (5), 8 profiles) × LS (Equation (7)) × CP (Year 1).

As for the cell size (5 m or 10 m), there are very little differences, not reflected in the areas classified by erosion risk. For the erosion risk classification, when carrying out the reclassification process, the values to be reclassified were closer to the classes used in methods 5 and 6, instead of all six classes of the scale. They only present four classes in

which the erosion risk varies from very low to severe, and not exceeding 100 t.ha^{-1} of annual soil losses, more specifically 77 t.ha^{-1}.year^{-1}. This class occurs occasionally for 0.12% of the basin, which seems to be closer to reality. Due to the better image resolution, a cell size of 5 was chosen to analyze the data.

3.1.1. R Factor

The average value of the erosivity factor (R) was calculated based on the average annual rainfall (P in mm.year^{-1}) recorded by the nearest meteorological station of [64] for the following time periods: 30 years, from 1981 to 2010; 10 years, from 2004 to 2013, the period used for SWAT modeling to generate climate data in statistical terms; and annually, for the 5 years of the study separately, which ran from 2009 to 2013, based on Equation (3). The values obtained are shown in Table 2 and Figure 5.

$$R = 2.23 \times P - 406.3, \quad (3)$$

Table 2. Average value of R based on values taken in meteorological stations near the study basin.

Years	1981–2010	2004–2013	2009	2010	2011	2012	2013
R (MJ. mm/h.ha.year)	896.85	1130.91	689.68	1406.02	2091.57	1532.28	2739.34

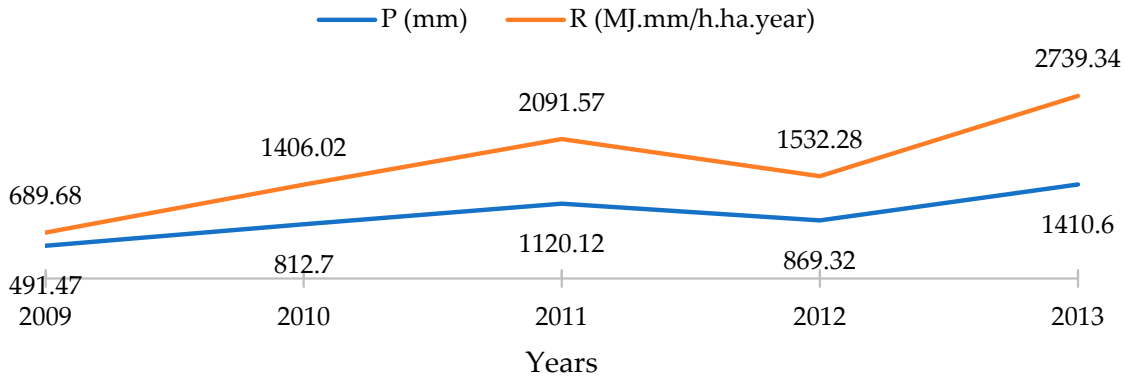

Figure 5. Variation of mean annual precipitation (P) and erosivity factor (R).

3.1.2. K Factor

The K factors are calculated for a period of 15 days by intervening the characteristics of the soils that enter their calculation, and then adjusted each day by interfering only with the moisture content. The procedure for calculating this factor is in accordance with [33,58]. Two methods were used to obtain K following the equations based on particle size percentages of soils around organic matter (f_{om}), sand (f_{sand}), silt (f_{silt}), and clay portions (f_{clay}): Equation (4), proposed by [65], and Equation (5), proposed by [66]. Figure 6a,b show the K factor distribution through the basin.

$$K = f_{silt-sand} \times f_{silt-clay} \times f_{om} \times f_{sand}, \quad (4)$$

$$K = \frac{-0.00043 \times (f_{silt-sand} + f_{silt})}{f_{om} + 0.000437 \times f_{sand} + 0.000863 \times f_{silt}}, \quad (5)$$

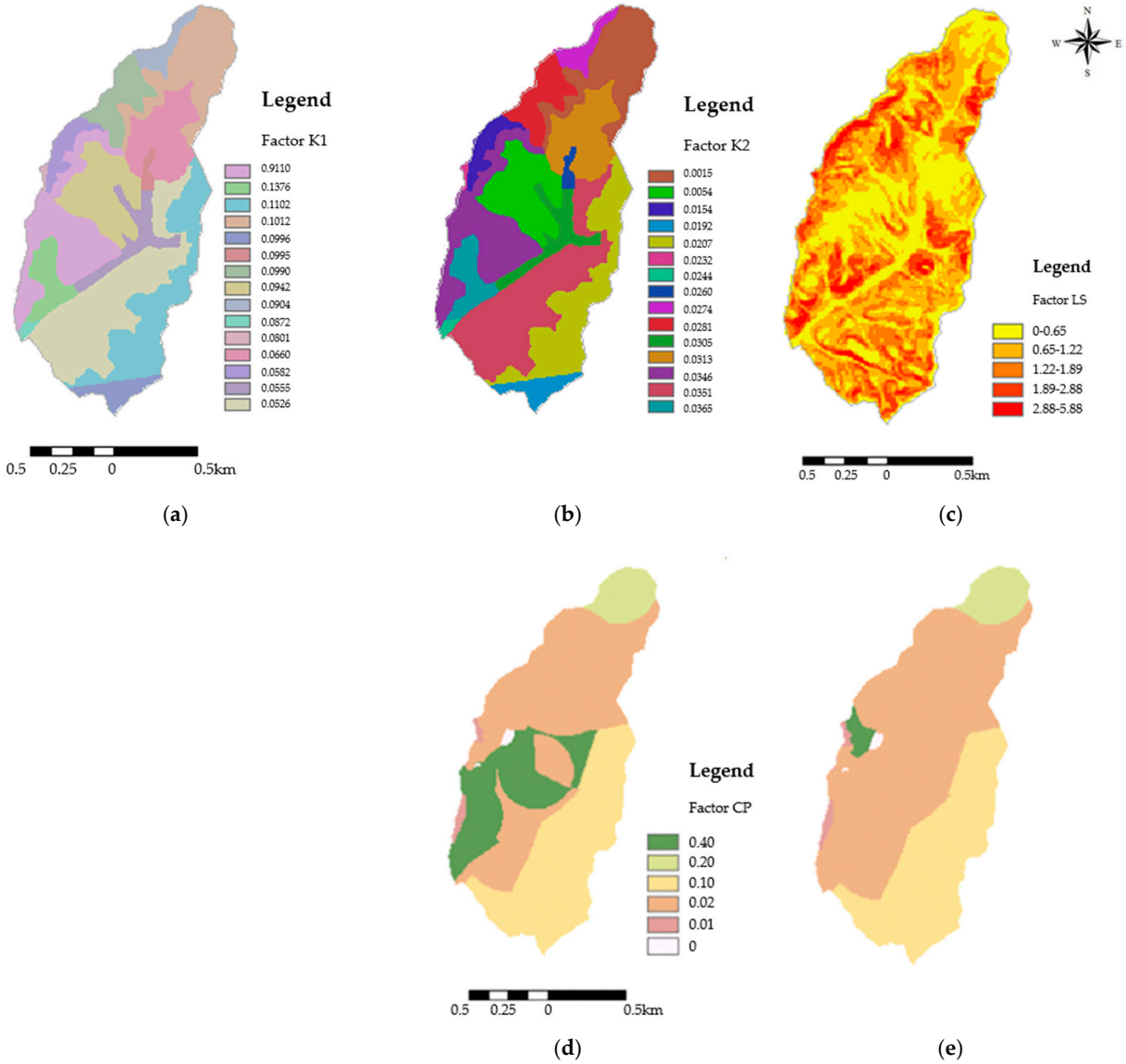

Figure 6. Distribution of K factor according to [65] (**a**), [66] (**b**), LS by [67] (**c**), and CP for the 1st (**d**) and 4th years (**e**).

3.1.3. LS Factor

Figure 6c shows the LS factor distribution through the basin. This study or physiographic factor was generated from the DEM, according to "standard" procedures in ArcGIS 10.8, "Spatial Analyst", according to Equation (6). Another method was used to obtain LS following equations based on terrain slope (slope in %) following Equation (7) by [67].

$$LS = \left[\left(\frac{FlowaccGrid}{22.13}\right)^{0.4}\right] \times 1.4\left[\left(\frac{SlopeGrid.sin}{0.0896}\right)^{1.3}\right], \quad (6)$$

$$LS = 1.822544 \times \left(\frac{slope}{8.96}\right)^{1.3} \quad (7)$$

3.1.4. CP Factor

Figure 6d,e show the CP factor distribution through the basin. Taking into account the graphic resolution of the maps, and by analyzing the results of Table 2, the following method of calculating the factors of the RUSLE was chosen: Method 6, with one dimension

of the cell of 5 corresponding to Equation (5) [66]; and for the K factor, Equation (7) [67]. It was also decided to use only one profile per soil patch (eight profiles) to calculate the K factor, since the values are not very different between method 5, which uses all the profiles, and method 6, which uses part of them (one per spot).

Considering the studied period, Figure 7 shows that the erosion risk class that occupies the largest area of the sub-basin is the one with losses below 5 t.ha^{-1}.year^{-1}, which means a very low risk of erosion, followed by the 5–12 t.ha^{-1}.year^{-1} class, with low erosion risk, and the moderate risk, with potential annual soil losses of 12–50 t.ha^{-1}.year^{-1}. The others were not representative.

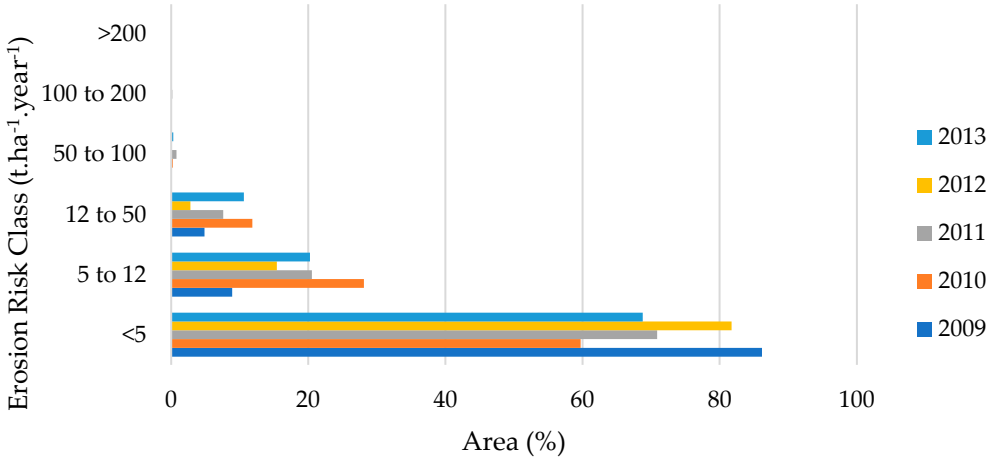

Figure 7. Representation of potential erosion risk classes according to [68].

Regarding the average soil losses by soil type, shown in Figure 8, there are higher average and maximum soil losses, in a generic way, in hydromorphic Fluvisols, followed by Luvisols, Cambisols, and the nonhydromorphic Fluvisols. Those results are not transversal for all the years, but mainly for the last two (2012 and 2013). This indicates that the results are mangled by the other factors, and it is not possible to attribute a direct relationship between the type of soil and soil losses.

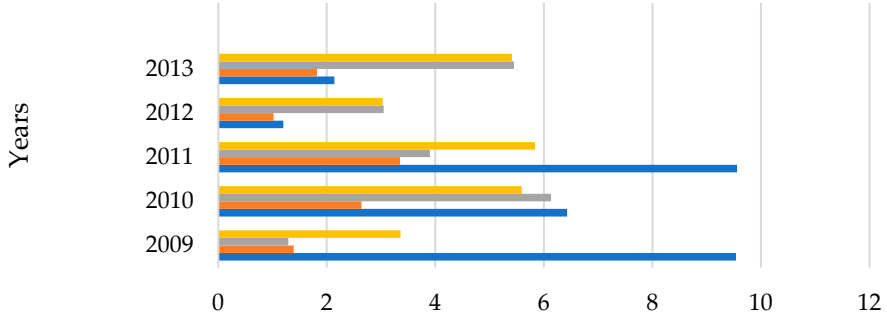

	2009	2010	2011	2012	2013
Luvisols	3.36	5.59	5.84	3.03	5.41
Cambisols	1.29	6.13	3.9	3.05	5.45
Fluvisols	1.39	2.64	3.35	1.02	1.82
Fluivisols Hydro.	9.54	6.43	9.56	1.2	2.14

Soil Losses (t.ha^{-1}.year^{-1})

Figure 8. Average soil losses according to soil type (2009 to 2013).

3.2. SWAT

With the introduction of the DEM, SWAT generated 25 hydrographic sub-basins, shown in Figure 9a, channeling the flow to the basin outlet, where the flow monitoring equipment and sediment measurement probe are located. With the information on occupation and soil type, 312 hydrological response units (HRUs) were generated and represented in Figure 9b.

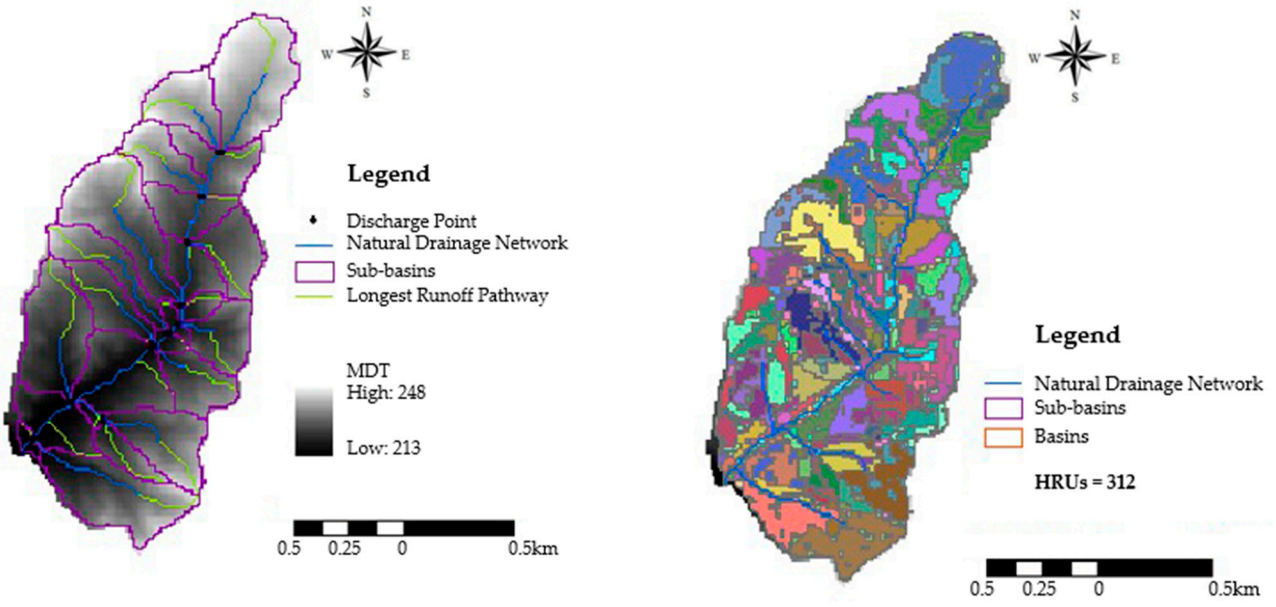

Figure 9. Sub-basins (25) with SWAT model with DEM (MDT) variation (**a**) and HRU (312) (**b**).

After the SWAT model described in the previous chapter, the model was run and obtained several output parameters, namely, the flow and the production of sediments, showed in Figure 10. In 2013, the highest flow occurred and the average annual precipitation reached the highest, which generated a greater production of sediments, shown in Figure 11. In 2012, the lowest sediment production was recorded, despite 2009 being the year with the lowest rainfall. According to Figure 11, the curves show the same trend; however, the SWAT model generated a lower production of sediments compared to the RUSLE model. The only exception was 2013, when the value was higher for the SWAT model.

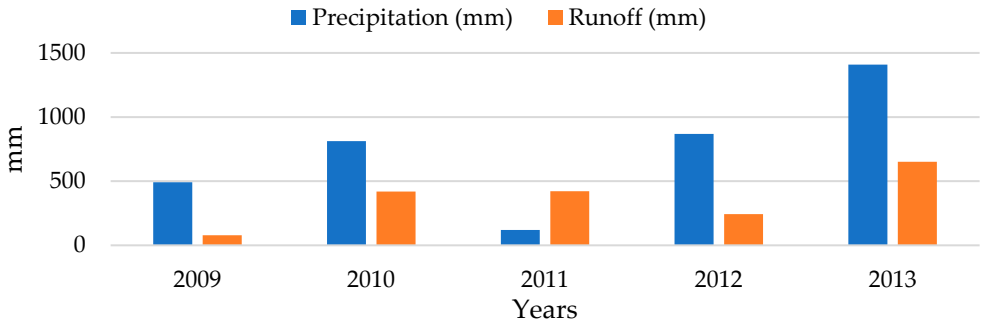

Figure 10. SWAT model results for the runoff and annual precipitation values.

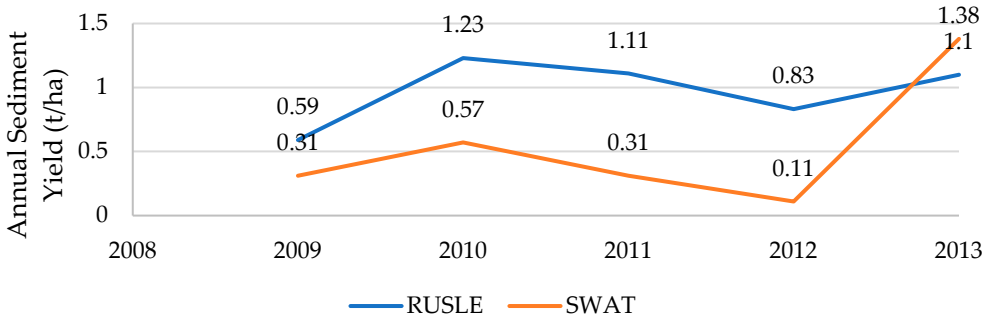

Figure 11. Simulated annual sediment production generated by SWAT and RUSLE models.

Statistical analysis was also performed within efficiency coefficient (EC) [69], comparing the simulated data in the SWAT model with those observed in the hydrometric and water quality station. This coefficient can vary from negative infinity to 1, with the value 1 indicating a perfect fit [70]. When the value is greater than 0.75, the model's performance is considered good; in between 0.36 and 0.75, it is acceptable; while a value lower than 0.36 is characterized as unacceptable [71].

The results for the runoff comparison were 0.49 and 0.38 for the sediments, which, according to EC, are characterized as qualified results. It should be noted that for the application of the EC, randomly observed data from a few days were selected for all the years in which the runoff and sediment measures were carried out. It can be concluded that the SWAT model, according to the application of the EC, is considered acceptable.

4. Discussion

Along with the research, soils were classified in the studied watershed, according to pedological and geotechnical classifications, identified as Cambisols, Fluvisols, and Luvisols. This detailed analysis provided insights into the properties of soils at different layers, highlighting significant differences, particularly in the Luvisols.

Subsequently, erosion models, RUSLE and SWAT, were applied to assess areas at higher risk of erosion within the sub-basin. RUSLE indicated annual variations in rainfall erosivity, with 2013 showing the highest indices, estimating soil loss ranging from 2.73 to 5.69 $t.ha^{-1}.year^{-1}$ during the period. Those values reflect a variable sediment production, identifying that erosion risks were mostly low, with occasional moderate risks. Even considering the worst hydrological cycle, the studied area will continue to have low to moderate risk, even considering the climate scenario predictions of [72], who indicated a 30 to 66% water erosion increase by 2070.

The SWAT, although underestimating sediment production compared to RUSLE, was deemed acceptable regarding statistical analysis using the Nash and Sutcliffe [69] EC calculation. The simulations demonstrated that changes in land use, particularly the reduction in annual crops, could significantly reduce sediment production, suggesting that land use management could be an effective strategy for mitigating erosion. A similar analysis was conducted by [73], where, in order to validate the model, they used machine learning (ML) and decision tree algorithms, reaching similar effectiveness with boosted tools. The use of ML, Internet of Things (IoT), and artificial intelligence (AI) seem to be the future of science as tools to power up the usual methods. Further research in the here-studied area is being carried out using ML-IoT-AI interaction to support decisionmakers. In addition, other variation and deep investigation should be centered around the RUSLE factors specifically. The authors of [74] approached only the erosivity factor (R) for Europe and calibrated it according to regional specifications. In addition, the authors of [75] improved the erodibility factor (K) according to soil texture determination methods, justifying that all other factors and methodologies can have those adjustments regarding model calibration.

Finally, the data resulted in the development of maps indicating erosion susceptibility and suitability for construction and material extraction, which revealed areas of varying

degrees of suitability and highlighted the limitations imposed by the agricultural nature of the region; these aspects are discussed as the following topic. This study corroborates others [76,77] that used empirical soil erosion models due to simplicity, and requires few resources to assess data for decisionmakers' support.

4.1. Susceptibility Charts

Three areas with erosion risk were identified in the water erosion susceptibility chart (Figure 12a) and are described below: 5 t.ha^{-1}.year^{-1}for very low erosion risk class (60 to 86%); 5 to 12 t.ha^{-1}.year^{-1}for low erosion risk class (9 to 28%); and 12 to 50 t.ha^{-1}.year^{-1} for moderate risk class (3 to 12%). The other classes for the period studied were not very significant or were nonexistent. For very specific situations, average soil losses of 50 to 100 tons occurred.

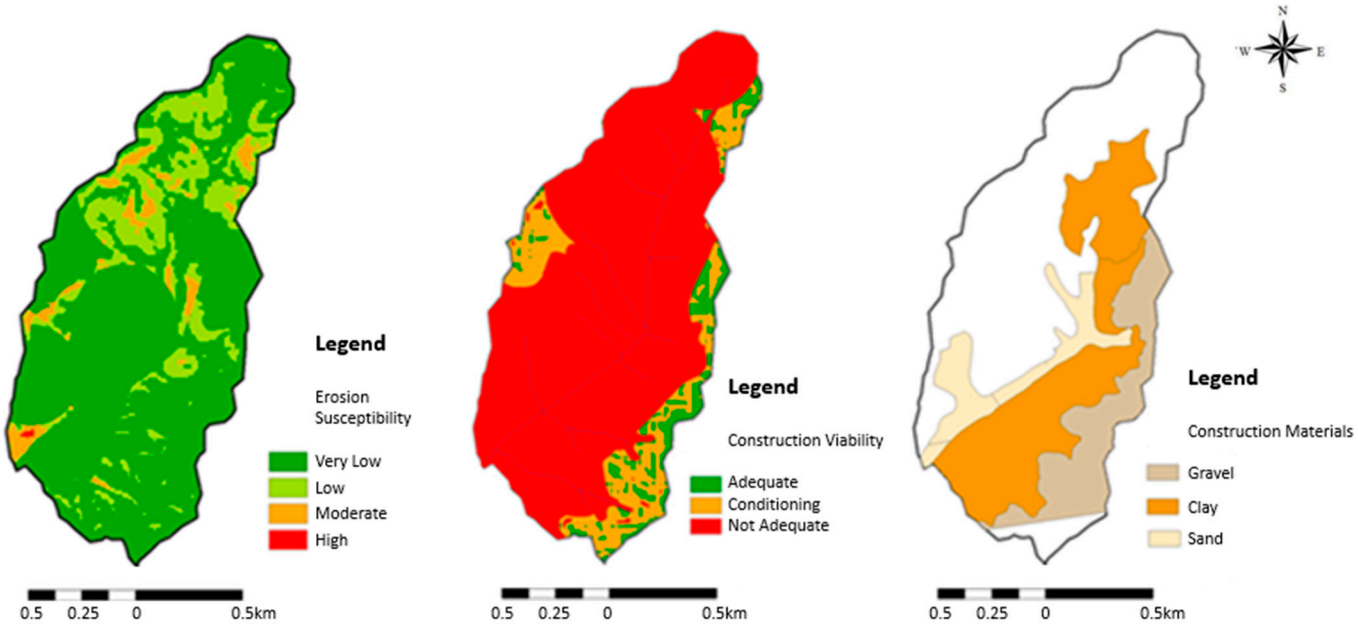

(**a**) (**b**) (**c**)

Figure 12. Charts of soil erosion susceptibility (**a**), construction suitability (**b**), and materials disponible for industries (**c**).

In the construction suitability chart (Figure 12b), three zones were considered: one green, with good suitability; another orange, conditioned; and red, not suitable. For its construction, algebraic operations were carried out in ArcGIS using the available cartography (soil type, DEM, slope distribution chart, geotechnical units, irrigation, 10 m protection strip on natural drainage network with reservoirs, and land occupation). By observing the map, there are few green areas of the sub-basin, which was expected, because it is a basin located in an agricultural area, leading to few area options. The construction materials chart exposes the areas of possible extraction of materials for industry (Figure 12c), especially around geotechnical and civil construction, indicating three areas with different materials that are capable of being used due to their characteristics. Those materials were verified through laboratory analyses, but are basically types of soil, in smaller proportions of gravels and sands, highlighting the quantity of clays.

4.2. Geotechnical Materials Frameworks

Susceptibility charts developed for the region studied show high material availability linked to very few areas for construction, justifying the agricultural aspect of the area. Furthermore, those results highlight the potential of the Portuguese countryside's economical side in providing raw materials for geotechnical and civil structures, due to the availability

of gravels, sands, and clays. Their use is very important geotechnically [78], where gravels are used in base layers to provide stability and drainage [79], filtering and preventing erosion; sands are used for asphalt, cement, or mortars mixtures [80]; and clays are used for bricks and core impermeabilization and sealing, preventing leakage and groundwater contamination [81–83].

Soils as raw materials are very important for earthworks, like roads and highways, crucial for cities' transportation and access [81]; bridges and tunnels, which enable efficient travel over obstacles like rivers and mountains; dams and reservoirs for water storage, flood control, irrigation, and hydroelectric power generation [82]; buildings, which provide shelter, workplaces, and are essential for urban development [83]; airports, for global connectivity and economic growth; railways, for mass transportation of people and goods, reducing road congestion and carbon emissions [84]; water supply systems for public health, sanitation, and access to clean water; and landfilling for waste management and environmental protection [85]. Overall, gravel, sands, and clays are indispensable in civil engineering and construction, forming the backbone of modern infrastructure and playing a pivotal role in societal development and sustainability [86].

Thus, their importance for society is summarized by economic growth, public health and safety, connectivity, energy and resources, urbanization, and development. Our research highlights the importance of monitoring and characterizing rural areas through soil erosion models, looking to provide a sustainable and resilient environmental development. This idea is linked to the United Nations Agenda [87] and the Sustainable Development Goals (SDG), with special focus on SDG3—Good Health and Well-Being, SDG6—Clean Water and Sanitation, SDG9—Industry, Innovation and Infrastructure, and SDG12—Responsible Consumption and Production.

5. Conclusions

The results of this study indicate that the SWAT model generates less sediment production in comparison with the RUSLE, being considered as more acceptable than SWAT, although an underestimation of results was present. In addition, the erosion risk class that predominated in the sub-basin was the one with losses of less than 5 $t.ha^{-1}.year^{-1}$ (60 to 86%), which means a very low risk of erosion, followed by the class with low erosion risk (9 to 28%), and moderate risk (3 to 12%). On the other hand, the SWAT model presented the highest runoff, annual average, and greater sediment production throughout the evaluated years.

The application and interpretation of those methods for the studied area could provide a better understanding of the land. Attaching that knowledge to society necessities, valuable data are generated to support decision-making agents to improve sustainable and resilient growth. Further studies could explore more field tests enlarging the studied area, and work with different erosion models to assess their potential and subsequent use, as soil is a necessary resource for the preservation of human life.

Author Contributions: Conceptualization, A.P.L., A.C.D., L.M. and V.C.; methodology, A.P.L., A.C.D., L.M. and V.C.; software, A.P.L.; validation, A.P.L., A.S. and M.V.M.; formal analysis, A.P.L. and A.C.D.; investigation, A.P.L., L.M., A.S. and M.V.M.; resources, A.C.D. and V.C.; data curation, A.P.L. and L.M.; writing—original draft preparation, A.P.L. and L.M.; writing—review and editing, L.M., A.C.D., A.S., M.V.M. and V.C.; visualization, A.C.D. and V.C.; supervision, V.C.; project administration, V.C.; funding acquisition, V.C. All authors have read and agreed to the published version of the manuscript.

Funding: The authors acknowledge the support by the GeoBioTec Research Unit, through the strategic projects UIDB/04035/2020 (https://doi.org/10.54499/UIDB/04035/2020) and UIDP/04035/2020 (https://doi.org/10.54499/UIDP/04035/2020), funded by the Fundação para a Ciência e a Tecnologia, IP/MCTES (Portugal) through national funds (PIDDAC).

Data Availability Statement: The authors declare that the data are unavailable due to privacy restrictions.

Conflicts of Interest: The authors declare no conflicts of interest.

References

1. Chen, W.; Huang, Y.; Lebar, K.; Bezak, N. A systematic review of the incorrect use of an empirical equation for the estimation of the rainfall erosivity around the globe. *Earth Sci. Rev.* **2023**, *238*, 104339. [CrossRef]
2. Garcia-Rodeja, E.; Macias, F.; Ojea, C. Reaccion com el FNa de los suelos da Galícia. I. Características y significado del teste de FNa. Distribuicion de la reatividade en funcion del material de partida. *An. Edafol. Agrobiol.* **1984**, *43*, 755–776.
3. Batista, P.V.; Davies, J.; Silva, M.L.; Quinton, J.N. On the evaluation of soil erosion models: Are we doing enough? *Earth-Sci. Rev.* **2019**, *197*, 102898. [CrossRef]
4. FAO. *El estado Mundial de la Agricultura y la Alimentacion 1994. Dilemas del Desarrollo y las Politicas Forestales*; Food & Agriculture Organization: Rome, Italy, 1994.
5. Veron, S.R.P.J.M.; Oesterheld, M. Assessing desertification. *J. Arid Environ.* **2006**, *66*, 751–763. [CrossRef]
6. Gómez, J.A.; Giráldez, J.V.; Pastor, M.; Fereres, E. Effects of tillage method on soil physical properties, infiltration and yield in an olive orchard. *Soil Tillage Res.* **1999**, *52*, 167–175. [CrossRef]
7. Prosdocimi, M.; Cerdà, A. Tarolli, Soil water erosion on Mediterranean vineyards: A review. *Catena* **2016**, *141*, 1–21. [CrossRef]
8. Zhidkin, A.; Gennadiev, A.; Fomicheva, D.; Shamshurina, E.; Golosov, V. Soil erosion models verification in a small catchment for different time windows with changing cropland boundary. *Geoderma* **2023**, *430*, 116322. [CrossRef]
9. Ye, B.; Chen, Y.; Li, Y.; Li, H.; Yang, L.; Wang, W. Risk assessment and water safety plan: Case study in Beijing, China. *J. Water Health* **2015**, *13*, 510–521. [CrossRef]
10. Casalí, J.; Gastesi, R.; Álvarez-Mozos, J.; De Santisteban, L.M.; de Lersundi, J.D.V.; Giménez, R.; Donézar, M. Runoff, erosion, and water quality of agricultural watersheds in central Navarre (Spain). *Agric. Water Manag.* **2008**, *95*, 1111–1128. [CrossRef]
11. Li, P.; Zhang, K.; Ling, P.; Zhao, L. Sediment transport capacity equation for soils from the Loess Plateau and northeast China. *Catena* **2023**, *223*, 106929. [CrossRef]
12. Troeh, F.R.; Hobbs, J.A.; Donahue, R.L. *Soil and Water Conservation: Productivity and Environmental Protection*; Prentice Hall Inc.: Hoboken, NJ, USA, 1999.
13. Diário da República. *Lei da Água. Lei n.º 58/2005. Diário da República n.º249/2005, Série I-A de 2005-12-29*; Diário da República: Lisbon, Portugal, 2005.
14. Lal, R. Soil erosion and the global carbon budget. *Environ. Int.* **2003**, *29*, 437–450. [CrossRef] [PubMed]
15. Efthimiou, N. Object-oriented soil erosion modelling: A non-stationary approach towards a realistic calculation of soil loss at parcel level. *Catena* **2023**, *222*, 106816. [CrossRef]
16. Oldeman, L.R. Global Extent of Soil Degradation. In *Bi-Annual Report*; ISRIC: Wageningen, The Netherlands, 1992.
17. Azevedo, J.C.R.D.; Nozaki, J. Análise de fluorescência de substâncias húmicas extraídas da água, solo e sedimento da Lagoa dos Patos-MS. *Química Nova* **2008**, *31*, 1324–1329. [CrossRef]
18. FAO. *World Reference Base for Soil Resources*; FAO World Soil Resources Report 84; Food and Agriculture Organization of United Nations: Rome, Italy, 1998.
19. Cortês, N.; Abreu, M.M. Solo—Recurso natural a preservar. In *Solo: A Pele da Terra*; Departamento de Geologia FCUL: Lisboa, Portugal, 2008.
20. Jabbour, C.J.C.; Fiorini, P.D.C.; Wong, C.W.; Jugend, D.; Jabbour, A.B.D.L.S.; Seles, B.M.P.R.; da Silva, H.M.R. First-mover firms in the transition towards the sharing economy in metallic natural resource-intensive industries: Implications for the circular economy and emerging industry 4.0 technologies. *Resour. Policy* **2020**, *66*, 101596. [CrossRef]
21. Jetten, V.; De Roo, A.D.; Favis-Mortlock, D. Evaluation of field-scale and catchment-scale soil erosion models. *Catena* **1999**, *37*, 521–541. [CrossRef]
22. Gonzales-Romero, J.; Zema, D.; Carrà, B.; Neris, J.; Fajardo, A.; Plaza-Álvarez, P.; Moya, D.; Peña-Molina, E.; Heras, J.; Lucas-Borja, M. Soil erosion modelling of burned and mulched soils following a Mediterranean forest wildfire. *Soil Use Manag.* **2022**, *39*, 881–899. [CrossRef]
23. Bai, Y.; Cui, H. An improved vegetation cover and management factor for RUSLE model in prediction of soil erosion. *Environ. Sci. Pollut. Res.* **2021**, *28*, 21132–21144. [CrossRef]
24. Morgan, R.P.C.; McIntyre, K.; Vickers, A.W.; Quinton, J.N.; Rickson, R.J. A rainfall simulation study of soil erosion on rangeland in Swaziland. *Soil Technol.* **1997**, *11*, 291–299. [CrossRef]
25. Abdelsamie, E.; Abdellatif, M.; Hassan, F.; El Baroudy, A.; Mohamed, E.; Kucher, D.; Shokr, M. Integration of RUSLE Model, Remote Sensing and GIS Techniques for Assessing Soil Erosion Hazards in Arid Zones. *Agriculture* **2023**, *13*, 35. [CrossRef]
26. Gonçalves, V.; Albuquerque, A.; Almeida, P.G.; Cavaleiro, V. DRASTIC Index GIS-Based Vulnerability Map for the Entre-os-Rios Thermal Aquifer. *Water* **2022**, *14*, 2448. [CrossRef]
27. Cronshey, R.G.; Theurer, F.D. AnnAGNPS-non point pollutant loading model. In Proceedings of the First Federal Interagency Hydrologic Modeling Conference, Las Vegas, NV, USA, 19–23 April 1998.
28. Arnold, J.G.; Allen, P.M. Estimating hydrologic budgets for three Illinois watersheds. *J. Hydrol.* **1996**, *176*, 57–77. [CrossRef]
29. Knisel, W.G.; Moffitt, D.C.; Dumper, T.A. Representing seasonally frozen soil with the CREAMS model. *Trans. ASAE* **1985**, *28*, 1487–1493. [CrossRef]
30. Laflen, J.M.; Elliot, W.J.; Flanagan, D.C.; Meyer, C.R.; Nearing, M.A. WEPP-predicting water erosion using a process-based model. *J. Soil Water Conserv.* **1997**, *52*, 96–102.

31. Williams, J.R.; Renard, K.G. Assessments of soil erosion and crop productivity with process models (EPIC). In *Soil Erosion and Crop Productivity*; American Society Agronomy: Madison, WI, USA, 1985; pp. 67–103.
32. Wischmeier, W.H.; Smith, D.D. *Predicting Rainfall Erosion Losses: A Guide to Conservation Planning*; Department of Agriculture, Science and Education Administration: USDA, MD, USA, 1978; Volume 537.
33. Renard, K.G. *Predicting Soil Erosion by Water: A Guide to Conservation Planning with the Revised Universal Soil Loss Equation (RUSLE)*; United States Government Printing: Washington, DC, USA, 1997.
34. Smith, R.E.; Goodrich, D.C.; Quinton, J.N. Dynamic, distributed simulation of watershed erosion: The KINEROS2 and EUROSEM models. *J. Soil Water Conserv.* **1995**, *50*, 517–520.
35. Cavaleiro, V.M.P. Condicionantes Geotécnicas à Expansão do Núcleo Urbano da Covilhã. Ph.D. Thesis, Universidade da Beira Interior, Covilhã, Portugal, 2001.
36. Marchiori, L. Mechanical and Hydraulic Long-Term Behavior for an Experimental Compacted Liner Embankment. Master's Thesis, Universidade Beira Interior, Covilhã, Portugal, 13 December 2022.
37. da Silva, R.P.; Lacerda, W.A.; Coelho Netto, A.L. Relevant geological-geotechnical parameters to evaluate the terrain susceptibility for shallow landslides: Nova Friburgo, Rio de Janeiro, Brazil. *Bull. Eng. Geol. Environ.* **2022**, *81*, 57. [CrossRef]
38. Cerri, L. Carta geotécnica: Contribuições para uma concepção voltada as necessidades brasileiras. In *Congresso Brasileiro de Geologia e Engenharia*; ABGE: Salvador, Brazil, 1990.
39. Grant, K.; Finlayson, A.A. The PUCE System for terrain analysis, assessment and evaluation as used for urban and regional development. In Proceedings of the 5th Australian Conference on Urban and Regional Planning Information Systems (URPIS FIVE), Canberra, Australia, 9–11 November 1977.
40. Duarte, A.C.; Mateos, L. How changes in cropping intensity affect water usage in an irrigated Mediterranean catchment. *Agric. Water Manag.* **2022**, *260*, 107274. [CrossRef]
41. Bos, M.G.; Replogle, J.A.; Clemmens, A.J. *Flow Measuring Flumes for Open Channel Systems*; American Society of Agricultural Engineers: Joseph, MI, USA, 1984.
42. INAG. *National Programme for Dams with High Hydroelectric Potential Programa Nacional de Barragens com Elevado Potencial Hidroeléctrico (PNBEPH)*; General Directorate for Energy and Geology and National Transmission Operator: Lisbon, Portugal, 2007.
43. Ecossistema Lda. *IC31—Castelo Branco/Monfortinho. Estudo Prévio, III, Estudo de Impactes Ambientais, Peças Escritas, Relatório Tomo 2/3*; Estradas de Portugal (EP): Castelo Branco, Portugal, 2010.
44. Julivert, M.; Ribeiro, A. *Memória Explicativa del Mapa Tectónico de la Peninsula Iberica y Baleares*; Institute de Geología y Mineración de España: Madrid, Spain, 1974.
45. Ferreira, N.; Iglesias, M.; Noronha, F.; Pereira, E.; Ribeiro, A.; Ribeiro, M.L. *Granitóides da Zona Centro Ibérica e seu enquadramento geodinâmico. Geologia de los granitoides y rocas associadas del Macizo Hesperico*; Livro Homenagem; Instituto Geológico y Minero de España: Madrid, Spain, 1987; pp. 37–51.
46. Thadeu, D. *Nota Explicativa da Carta Geológica de Portugal na Escala de 1:1.000.000*; Serviço Geológico de Lisboa: Lisboa, Portugal, 1958.
47. Ribeiro, O. Sur la morphologie da la Basse Beira. *Bull. Assoc. Géographie Fr.* **1939**, *122*, 113–122. [CrossRef]
48. Ribeiro, O. Notas sobre a evolução morfológica da condilheira central. *Bol. Geológico Porto* **1942**, *1*.
49. Ribeiro, O. Evolução da falha Ponsul. *Comun. Dos Serviços Geol. Port.* **1943**, *XXIV*.
50. Ribeiro, O. Três notas de geomorfologia da Beira Baixa. *Comun. Dos Serviços Geol. Port.* **1951**, *XXXII*, 271–294.
51. Daveau, S. Structure et relief de la Serra da Estrela. *Finisterra* **1969**, *4*, 159–197.
52. Young, T.P. The lithostratigraphy of the Upper Odovician of Central Portugal. *J. Geol. Soc.* **1988**, *145*, 377–392. [CrossRef]
53. Cunha, P.P. O Terciário da Beira Baixa: Registo estratigráfico e interpretação paleogeográficas. *Geonovas* **2001**, *15*, 19–31.
54. Pereira, A.J.S.C.; Pereira, L.C.G.; Macedo, C.A.R. Os plutonitos da Zebreira: Idade e enquadramento estrutural. Memórias e Notícias. *Publicação Laboratório Miner.* **1986**, *101*, 21–31.
55. Corretge, L. Aspectos petrológicos y estruturales de las rocas filonianas en el Complejo Esquisto Grauváquico del área Zarza-la-Mayor. In Proceedings of the I Congreso Español de Geología, Segovia, Spain, 9–14 April 1984.
56. Sequeira, A. O grupo das Beiras (Complexo Xisto Grauváquico) entre Zebreira e Penamacor e a sua relação com o Ordovícico. In Proceedings of the III Congresso Nacional de Geologia, Lisboa, Portugal, 21–23 October 1991.
57. Bosch, D.; Theurer, F.; Bingner, R.; Felton, G.; Chaubey, I. Evaluation of the AnnAGNPS water quality model. In *Agricultural Non-Point Source Water Quality Models: Their Use and Application*; ASAE: Orlando, FL, USA, 1998; pp. 45–54.
58. Yuan, Y.; Bingner, R.L.; Theurer, F.D.; Rebich, R.A.; Moore, P.A. Phosphorus component in AnnAGNPS. *Trans. ASAE* **2005**, *48*, 2145–2154. [CrossRef]
59. Williams, J.R.; Arnold, J.G.; Kiniry, J.R.; Gassman, P.W.; Green, C.H. History of model development at Temple, Texas. *Hydrol. Sci. J.* **2008**, *53*, 948–960. [CrossRef]
60. Aksoy, H.; Kavvas, M.L. A review of hillslope and watershed scale erosion and sediment transport models. *Catena* **2005**, *64*, 247–271. [CrossRef]
61. Albuquerque, A.W.; Lombardi Neto, F.; Srinivasan, V.S.; Santos, J.R. Manejo da cobertura do solo e de práticas conservacionistas nas perdas de solo e água em Sumé, PB. *Rev. Bras. Eng. Agrícola Ambient.* **2002**, *6*, 136–141. [CrossRef]

62. van Griensven, A.V.; Meixner, T.; Grunwald, S.; Bishop, T.; Diluzio, M.; Srinivasan, R. A global sensitivity analysis tool for the parameters of multi-variable catchment models. *J. Hydrol.* **2006**, *324*, 10–23. [CrossRef]
63. Adriolo, M.V.; Santos, I.D.; Gibertoni, R.C.; Camargo, A.D. Calibração do modelo SWAT para a produção e transporte de sedimentos. *Simpósio Bras. Sobre Pequenas E Médias Centrais Hidrelétricas* **2008**, *6*, 1–18.
64. Agroconsultores. *Carta de Aptidão e Uso da Terra, Zona Interior Centro (ZIC)*; IDRHa—Instituto de Desenvolvimento Rural e Hidráulica: Lisboa, Portugal, 2003.
65. Williams, J. Chapter 25: The EPIC model. In *Computed Models of Watershed Hydrology*; Singh, V.P., Ed.; Water Resource Publication: Baton Rouge, LO, USA, 1995; pp. 909–1000.
66. Chaves, H.M.L. Modelagem Matemática da Erosão Hídrica: Passado, Presente e Futuro—O Solo nos Grandes Domínios Morfoclimáticos do Brasil e o Desenvolvimento Sustentado. Ph.D. Thesis, University of Viçosa, Minas Gerais, Brazil, 1996.
67. Moore, I.D.; Burch, G.J. Physical basis of the length-slope factor in the universal soil loss equation. *Soil Sci. Soc. Am. J.* **1986**, *50*, 1294–1298. [CrossRef]
68. Irvem, A.; Topaloglu, F.; Uygur, V. Estimating spatial distribution of soil loss over Seyhan River Basin in Turkey. *J. Hydrol.* **2007**, *336*, 30–37. [CrossRef]
69. Nash, J.E.; Sutcliffe, J.V. River flow forecasting through conceptual models part I—A discussion of principles. *J. Hydrol.* **1970**, *10*, 282–290. [CrossRef]
70. ASCE. *Hydrologic Handbook, 2 ed.*; ASCE Manual and Report on Engineering Practice, 28; American Society of Civil Engineers: Reston, VA, USA, 1996.
71. Silva, P.; Mello, C.; Silva, A.; Coelho, G. Modelagem da Hidrógrafa de Cheia em uma Bacia Hidrográfica da Região Alto Rio Grande. *Rev. Eng. Agrícola Ambient.* **2008**, *12*, 258–265. [CrossRef]
72. Borrelli, P.; Robinson, D.; Panagos, P.; Lugato, E.; Yang, J.; Alewell, C.; Wuepper, D.; Montanarella, L.; Ballabio, C. Land use and climate change impacts on global soil erosion by water (2015–2070). *Proc. Natl. Acad. Sci. USA* **2020**, *117*, 21994–22001. [CrossRef] [PubMed]
73. Garrido, F.; Granda, P. Risk Analysis of Soil Erosion Using Remote Sensing, GIS, and Machine Learning Models in Imbabura Province, Ecuador. *SN Comput. Sci.* **2024**, *5*, 16. [CrossRef]
74. Panagos, P.; Ballabio, C.; Borrelli, P.; Meusburger, K.; Klik, A.; Rousseva, S.; Tadic, M.; Michaelides, S.; Hrabalíková, M.; Aalto, O.P.J.; et al. Rainfall erosivity in Europe. *Sci. Total Environ.* **2015**, *511*, 801–814. [CrossRef]
75. Komissarov, M.; Fomicheva, D.; Zhidkin, A.; Yudina, A. Variations in soil erodibility (K-factor) for the Chernozems depending on the method of texture determination. *MethodsX* **2024**, *13*, 102876. [CrossRef]
76. Ganasri, B.; Ramesh, H. Assessment of soil erosion by RUSLE model using remote sensing and GIS—A case study of Nethravathi Basin. *Geosci. Front.* **2016**, *7*, 953–961. [CrossRef]
77. Ghavami, M.; Ayobi, S.; Khaleghpanah, N.; Mosaddeghi, M.; Gohari, A. Soil loss estimation using RUSLE model: Comparison of conventional and digital soil data at watershed scale in central Iran. *Soil Tillage Res.* **2024**, *244*, 106238. [CrossRef]
78. Matos Fernandes, M. *Mecânica dos Solos*, 2nd ed.; FEUP: Porto, Portugal, 1995.
79. Seed, H.; Booker, J. Stabilization of potentially liquefiable sand deposits using gravel drains. *J. Geotech. Eng. Div.* **1977**, *103*, 757–768. [CrossRef]
80. Umar, H.; Zeng, X.; Lan, X.; Zhu, H.; Li, Y.; Liu, H. A Review on Cement Asphalt Emulsion Mortar Composites, Structural Development, and Performance. *Materials* **2021**, *14*, 3422. [CrossRef] [PubMed]
81. Laurance, W. Bad Roads, Good Roads. In *Handbook of Road Ecology*; Wiley: Hoboken, NJ, USA, 2015; Chapter 2.
82. Stajano, F.; Hoult, N.; Wassel, I.; Bennet, P.; Middleton, C.; Soga, K. Smart bridges, smart tunnels: Transforming wireless sensor networks from research prototypes into robust engineering infrastructure. *Ad Hoc Netw.* **2010**, *8*, 872–888. [CrossRef]
83. Marcus, C.F.C. *People Places: Design Guidelines for Urban Open Space*, 2nd ed.; John Wiley & Sons, INC.: Toronto, ON, Canada, 1997.
84. Addie, J.-P. Flying high (in the competitive sky): Conceptualizing the role of airports in global city-regions through "aero-regionalism. *Geoforum* **2014**, *55*, 87–99. [CrossRef]
85. Hunter, P.; MacDonald, A.; Carter, R. Water supply and health. *PLoS Med.* **2010**, *7*, e1000361. [CrossRef]
86. Marchiori, L.; Morais, M.V.; Studart, A.; Albuquerque, A.; Andrade Pais, L.; Ferreira Gomes, L.; Cavaleiro, V. Energy Harvesting Opportunities in Geoenvironmental Engineering. *Energies* **2024**, *17*, 215. [CrossRef]
87. United Nations Parliament and Council. *The 2030 Agenda for Sustainable Development*; UN: Geneva, Switzerland, 2020.